Electrogenerated Chemiluminescence

Robert J. Forster, Paolo Bertoncello, and Tia E. Keyes

Biomedical Diagnostics Institute, National Center for Sensor Research, School of Chemical Sciences, Dublin City University, Dublin 9, Ireland; email: Robert.Forster@dcu.ie, Paolo.Bertoncello@dcu.ie, Tia.Keyes@dcu.ie

Annu. Rev. Anal. Chem. 2009. 2:359–85

First published online as a Review in Advance on March 18, 2009

The *Annual Review of Analytical Chemistry* is online at anchem.annualreviews.org

This article's doi:
10.1146/annurev-anchem-060908-155305

1936-1327/09/0719-0359$20.00

Key Words

emission, ruthenium polypyridyl, metal complexes, electroanalysis, sensors

Abstract

In electrogenerated chemiluminescence, also known as electrochemiluminescence (ECL), electrochemically generated intermediates undergo a highly exergonic reaction to produce an electronically excited state that then emits light. These electron-transfer reactions are sufficiently exergonic to allow the excited states of luminophores, including polycyclic aromatic hydrocarbons and metal complexes, to be created without photoexcitation. For example, oxidation of $[Ru(bpy)_3]^{2+}$ in the presence of tripropylamine results in light emission that is analogous to the emission produced by photoexcitation. This review highlights some of the most exciting recent developments in this field, including novel ECL-generating transition metal complexes, especially ruthenium and osmium polypyridine systems; ECL-generating monolayers and thin films; the use of nanomaterials; and analytical, especially clinical, applications.

1. INTRODUCTION

Electrochemiluminescence (ECL) was first identified in the 1960s through the use of rubrene, 9,10-diphenylanthracene (DPA), and related compounds (1, 2). Then in the 1970s, ECL was observed by reacting electrogenerated tris-2,2′-bipyridylruthenium(III) $[Ru(bpy)_3]^{3+}$ (where bpy refers to 2,2′-bipyridine) with tripropylamine (TPA) to create an electronically excited state that emits at approximately 610 nm (3). ECL has several attractive features, including absence of a background optical signal, precise control of reaction kinetics offered by controlling the applied potential, compatibility with solution-phase and thin-film formats, and opportunities to enhance intensity with nanomaterials such as metallic nanoparticles and nanotubes. Together, these features make ECL a highly sensitive and selective analytical method. For example, ECL-generating species have been used extensively as labels on biological molecules, allowing many clinically relevant analytes to be determined at subpicomolar concentrations via conventional antibody or nucleic acid assay approaches. Currently, intense research is under way to identify new luminophores, film formations, mechanistic studies, and analytical applications. Several excellent reviews covering ECL have been published (4–12).

2. ELECTROGENERATED CHEMILUMINESCENCE–GENERATION PATHWAYS

2.1. Overview

There are two dominant pathways through which ECL can be produced, namely the annihilation and coreactant pathways. In each case, two species are generated electrochemically, and those two species undergo an electron-transfer reaction to produce an emissive species.

2.2. Annihilation Pathway

In the annihilation pathway, two species are electrochemically generated; for instance, oxidized and reduced forms of the luminophore are produced within the depletion zone by a potential step or sweep. These species then interact to produce both a ground state and an electronically excited state, which then relaxes by emission. For example, as demonstrated in Equations 1–4, the electrochemically generated anion and cation radicals of DPA recombine to form one ground-state DPA and one excited-state *DPA:

$$DPA \rightarrow DPA^+ + e^-, \text{ electrochemical step occurring at } E_1^{\circ\prime}, \quad (1)$$

$$DPA + e^- \rightarrow DPA^-, \text{ electrochemical step occurring at } E_2^{\circ\prime}, \quad (2)$$

$$DPA^- + DPA^+ \rightarrow DPA + {}^*DPA, \quad (3)$$

$${}^*DPA \rightarrow DPA + \text{emission at approximately 425 nm}. \quad (4)$$

The corresponding free energy for the annihilation reaction, ΔG, can be determined with Equation 5:

$$\Delta G = nF(E^\circ_{Donor} - E^\circ_{Acceptor}), \quad (5)$$

where E°_{Donor} and $E^\circ_{Acceptor}$ are the formal potentials for the ground-state reduction and oxidation processes, respectively. Given that these values are +1.4 and –1.7 V, ΔG is of the order of –3.1 eV. The wavelength of maximum emission obtained for the DPA at 77 K following photoexcitation

is 2.8 eV. Therefore, the free energy of the annihilation reaction exceeds that required to create the electronically excited state, and ECL becomes possible. In this sense, the reaction is energy sufficient because the free energy of the reaction is greater than or equal to the energy of the emissive state. For DPA, an excited-state singlet is created, and this process is known as the singlet route (S-route).

However, some pivotal ECL reactions occur from a triplet state (13). For example, many ECL-based assays rely on ruthenium tris-bipyridyl–type systems:

$$[Ru(bpy)_3]^{2+} \rightarrow [Ru(bpy)_3]^{3+} + e^-,\ E^{\circ\prime} = +1.2\ V, \tag{6}$$

$$[Ru(bpy)_3]^{2+} + e^- \rightarrow [Ru(bpy)_3]^{+},\ E^{\circ\prime} = -1.4\ V, \tag{7}$$

$$[Ru(bpy)_3]^{3+} + [Ru(bpy)_3]^{+} \rightarrow [Ru(bpy)_3]^{2+} + [Ru(bpy)_3]^{2+*}, \tag{8}$$

$$[Ru(bpy)_3]^{2+*} \rightarrow [Ru(bpy)_3]^{2+} + \text{photon}\ (\lambda_{max} = 610\ nm \equiv 2.1\ eV). \tag{9}$$

An advantage of the annihilation pathway is that it requires only the electrochemiluminescent species, solvent, and supporting electrolyte to generate light. However, the potential window of water is often not sufficiently wide to allow the luminophore to be both oxidized and reduced, making it necessary to use organic solvents such as acetonitrile and *N*,*N*-dimethylformamide.

2.3. Coreactant Pathway

Cross-reactions involving dissimilar species, such as an ECL generator and a coreactant, often involve triplet–triplet annihilation. For example, the electrochemically generated anion radical of DPA and the cation of *N*,*N*,*N**,*N**-tetramethyl-*p*-phenylenediamine (TMPD) react to form a DPA triplet and TMPD. Two DPA triplets then undergo an annihilation reaction to form a DPA ground state and a singlet excited state, which then emits at approximately 425 nm. This scheme is significant because the initial DPA–TMPD reaction is energy deficient: It does not have enough energy to generate the excited state.

A key advantage of the coreactant approach is that it facilitates ECL generation in aqueous solution, opening up a wide range of assays for molecules of diagnostic or biological relevance. In this approach, a species present in the solution, such as TPA (14), is either oxidized or reduced in the same potential step as the ECL species. Through electron transfers or chemical reactions that follow electron transfer, the coreactant generates a product that reacts with the ECL luminophore to generate an excited state. In the case of ruthenium-bpy-based ECL, amines—especially tertiary amines such as TPA—are the dominant coreactants. However, others include persulfate ion, which operates in the reductive-oxidation mode, and oxalate ion, which operates in the oxidative-reduction mode.

At least four distinct reaction mechanisms have been proposed for the coreactant pathway between ruthenium tris-bipyridyl and TPA (15, 16). However, there are some difficulties with these mechanisms; for instance, the lifetime of the R_3N^{*+} cation generated by oxidation seemed to be either too long on the basis of electron paramagnetic resonance measurements or too short on the basis of voltammetric measurements, wherein a reverse wave is absent and the peak potentials are much lower than the $E^{\circ\prime}$ values estimated from photoinduced electron-transfer measurements. Recently, Pastore and coworkers (17) discussed the possibility that for pH values less than 5, the deprotonation of the R_3NH^+ was the rate-limiting step, whereas above pH 5, the formation of an amine neutral radical was the rate-limiting step. This amine-neutral radical was hypothesized to be the

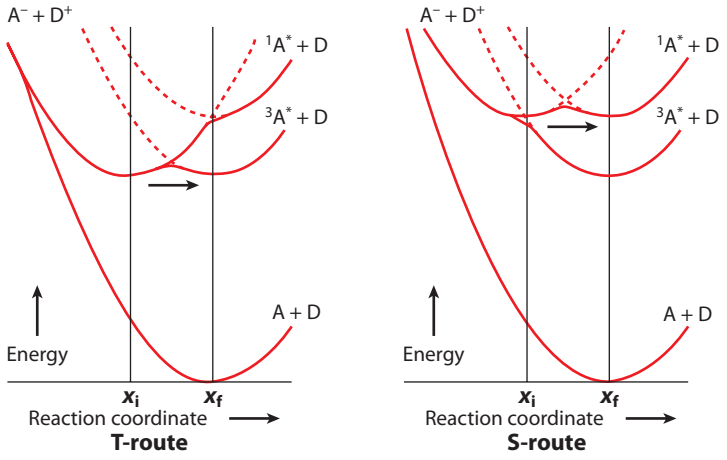

Figure 1

Reaction coordinate diagrams for electrochemiluminescence (ECL) processes occurring according to the triplet route (T-route) (*left*) and the singlet route (S-route) (*right*). Potential energy curves are presented in the zeroth-order (*dotted curves*) and first-order (*solid curves*) approximations, with degeneracy at the potential energy curve crossing points removed in the latter. Abbreviations: A, acceptor; D, donor. Reprinted with permission from Reference 18.

final end product of a chain of reactions starting with the oxidation of the deprotonated amine R_3N to R_3N^{+*}, the formation of an ion pair between R_3N^{+*} and HPO_4^{3-} (in phosphate buffer), and the eventual loss of a proton by R_3N^{+*} to form R_3N^*, which is the amine-neutral radical. The ion pair is hypothesized to be the species observed in electron paramagnetic resonance measurements.

A key feature of ECL is that the reaction is highly exergonic. For ruthenium tris-bipyridyl–based systems reacting with TPA, ΔG is of the order of –2.3 eV, and the reaction is expected to lie in the Marcus inverted region (18). However, although production of the ground-state species is highly exergonic, there are kinetically faster pathways that create excited states. **Figure 1** illustrates the reaction coordinate diagrams for ECL triplet route (T-route) and S-route pathways (18). The figure shows both the ground-state products and the excited-state products. Significantly, in both cases, the activation energy required to generate an excited-state product was lower than that required for a ground-state product.

This observation has significant implications for designing new ECL systems. For example, ECL efficiencies can be predicted using the Marcus theory, provided that the annihilation reaction occurs without other competitive reactions. A more complete approach would be to include the vibronic excitation in the reaction products, solvent molecule dynamics, and changes in the electron-transfer distance and medium separating the donor and acceptor. The electron-transfer distance dependence is especially important in designing new ECL systems because the donor and acceptor must be in close proximity for electron transfer to occur. The ability to control this donor–acceptor separation, at least on a statistical basis, is one of the attractive features of thin films and even monolayers of ECL species.

3. LUMINOPHORE DESIGN

3.1. Monomeric Complexes

The development of novel homo- and heteroleptic transition metal complexes continues to be an area of significant study. For example, the hydrophobicity, excited-state location within the

complex, luminescence lifetime, wavelength of maximum emission, and both ground- and excited-state redox potentials can be optimized for particular applications by changing the identity of the peripheral ligands (19–21). The ability to control these features directly affects the overall performance of assays. For example, longer excited-state lifetimes may lead to a brighter ECL response, making the assay more sensitive, and reducing the redox potentials may eliminate parasitic Faradaic reactions, thus making the assay more selective. However, due to the complexity of the ECL-generation process, the photoluminescence efficiency does not directly predict the ECL intensity. Moreover, there is often no obvious relationship between the photoluminescence quantum yield and the ECL intensity. For example, the photoemission efficiency of $[Ru(bpy\text{-}COOEt]_3^{2+}$ exceeds that of $[Ru(bpy)_3]^{2+}$, yet it does not generate intense ECL. In contrast, luminophores with lower photoluminescence quantum yields show higher ECL than does $[Ru(bpy)_3]^{2+}$.

3.2. Multicenter Luminophores

Researchers are devoting significant effort to the development of dimers and dendrimers, with the objective of having a brighter overall emission. However, this result may not correspond to higher emission intensity per emitting center. For example, 1,4-bis(4′-methyl-2,2′-bipyridin-4-yl)benzene (bphb) acts as a bridge between two ruthenium centers within the complex $[(bpy)_2Ru(bphb)Ru(bpy)_2]^{4+}$ (22). This dimeric species produced two- to three-fold more intense emission than did $[Ru(bpy)_3]^{2+}$ in aqueous and nonaqueous solution through both annihilation and coreactant approaches. Significantly, these and other investigations reveal that in order to achieve a brighter emission there must be weak electronic coupling between the metal centers. Other weakly coupling bridges have been explored, notably amino acids and peptides such as lysine (23). However, even in systems where the centers interact weakly, multimetallic systems typically yielded an increase in ECL intensity of only ~30% with respect to mononuclear compounds. This behavior arises from the fact that the upper limit of achievable intensity is determined by the quantum yield of the luminophore, but in the case of ECL, steps such as the rate of diffusion or heterogeneous electron transfer may limit the actual intensity obtained.

Further increasing the number of linked luminophores (e.g., within dendrimers) may offer an enhanced ECL response. For example, in antibody or nucleic acid assays, the overall brightness of the label may be more important to achieving low limits of detection even if the emitters are individually less efficient when forming part of the larger structure. For example, eight $[Ru(bpy)_3]^{2+}$ units have been immobilized at the periphery of a carbosilane dendrimer platform (24). ECL of the functionalized dendrimer was five times greater than that of a control monometallic species. **Figure 2** shows the application of such a dendrimer in a bioassay (25). However, it is important to note that multisite labeling, especially with large dyes, can result in the loss of biological activity of the molecules as well as in precipitation.

3.3. Bioconjugation

Ruthenium- and osmium polypyridine–type complexes continue to play a pivotal role in ECL-based assay development. This dominance is due to the nearly ideal reversible voltammetry and their attractive photophysical properties as well as the synthetic versatility of the polypyridine and related ligands. For example, **Figure 3** illustrates the attachment of *n*-hydroxysuccinimide ester or phosphoramadite functional groups to the bipyridine moieties that facilitate covalent attachment to biological molecules such as antibodies and DNA (7). This strategy has opened up many analytical applications whose sensitivities rival those achieved via photoluminescence or radiolabeling

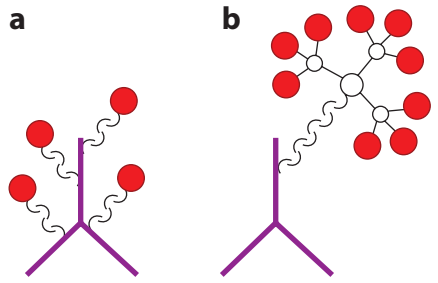

Figure 2

Labeling of a biomolecule at (*a*) multiple and (*b*) single sites using dendrimers. Reprinted with permission from Reference 25.

methods. Also, these reactive groups can be used to create monolayers of the luminophores on a wide variety of electrode surfaces, leading to the possibility of detecting antibodies labeled with a suitable coreactant (or nucleic acids can themselves act as the coreactant).

Beyond engineering the redox, photophysical, and binding properties of ECL luminophores, enhanced ECL can be achieved by making relatively subtle changes in the nature of the electrolyte solution. The best known of these changes is the addition of halide species (26). It is well known

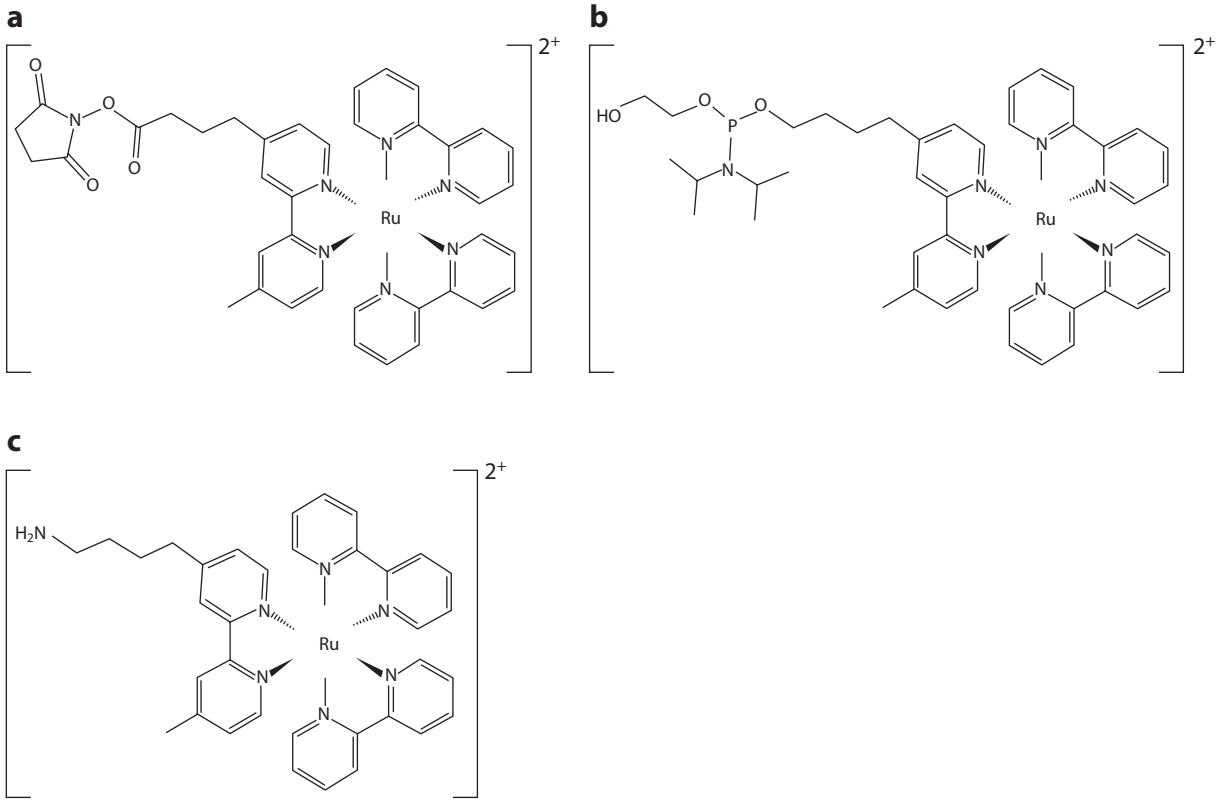

Figure 3

$[Ru(bpy)_3]^{2+}$-phosphoramadite (*a*), -maleimide (*b*), and -amine (*c*) for electrochemiluminescence labeling of biological molecules.

that the growth of surface oxides on platinum and gold electrodes is inhibited in the presence of halide, which increases the TPA oxidation current. Moreover, the dissolution of gold in halide-containing solutions, especially bromide, at positive potentials also activates the gold electrode surface, leading to enhanced ECL.

A difficulty frequently encountered in photoluminescence detection via ruthenium tris-bpy is quenching by dissolved oxygen. Significantly, this problem can be avoided in ECL generation. For example, in the cross-reaction pathway between $[Ru(bpy)_3]^{2+}$ and TPA (27), the emission intensity becomes independent of the oxygen concentration, provided that the TPA concentration exceeds the dissolved oxygen concentration. This behavior arises because electrogenerated TPA* reduces molecular oxygen, preventing it from quenching the electrochemiluminescent state.

4. INTERFACIAL MODIFICATION

4.1. Surfactant Addition

The addition of a surfactant can significantly increase the ECL efficiency. For example, adding a nonionic surfactant to the $[Ru(bpy)_3]^{2+}$/TPA coreactant system increases the ECL intensity by eightfold (28–30). Significantly, the enhancement mechanism appears to involve adsorption of surfactant on the electrode surface. As illustrated in **Figure 4**, the fluorosurfactant Zonyl FSN® resulted in a 50-fold-higher ECL intensity and a 400-mV negative shift in the oxidation potential. The fluorosurfactant apparently renders the electrode hydrophobic via adsorption of the hydrophilic polyethylene oxide group to the electrode, with the hydrophobic end oriented toward the solution. This physisorption process results in adsorption of $[Ru(bpy)_3]^{2+}$ and TPA close to the surface of the electrode. This observation opens up the possibility of achieving significantly enhanced ECL for suitably designed adsorbed species.

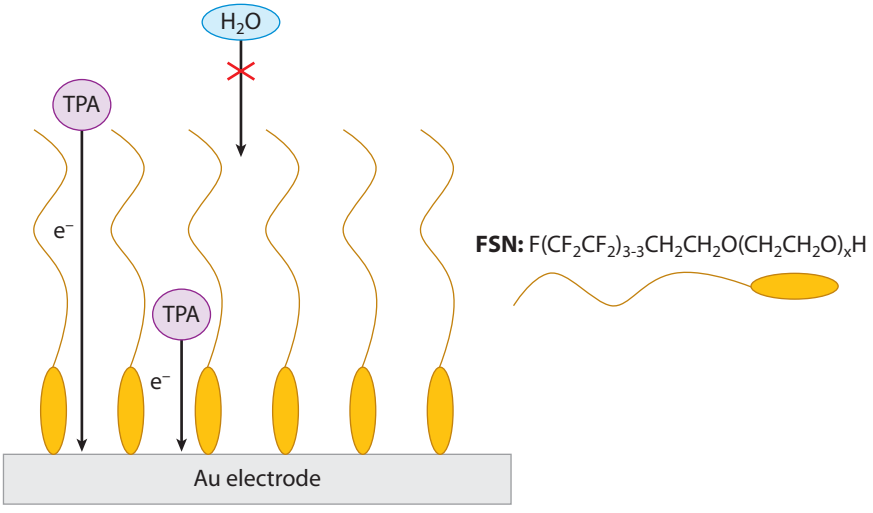

Figure 4

Adsorption of FSN molecules at a gold electrode. The adsorption precludes the access of H_2O to the electrode surface while facilitating the oxidation of tripropylamine (TPA). Reprinted with permission from Reference 31.

4.2. Adsorbed Monolayers

There are several disadvantages to the use of solution-phase reactants, including loss of signal due to diffusion of the ECL reagent out of the detection zone, the limited ability to repeatedly electrochemically cycle an individual luminophore, and high reagent consumption. To overcome these problems, considerable effort has been invested in immobilizing the $[Ru(bpy)_3]^{2+}$ reagent on an electrode. Several approaches have been developed, including direct attachment to the electrode as Langmuir–Blodgett films or self-assembled monolayers. Where the luminophore is not covalently linked to the electrode surface, it is challenging to unambiguously confirm that the emission arises from bound material rather than from a solution-based emission of leached surface material into the surrounding electrolyte.

The electrochemical, photophysical, and electrochemiluminescent properties of $[Ru(bpy)_2$dicarboxy-bpy$]^{2+}$ monolayers formed on optically transparent fluorine-doped tin oxide (FTO) electrodes have been reported (32). The surface coverage of the complex was 2.5×10^{-10} mol cm^{-2}, which is consistent with the coverage expected for a close-packed monolayer. The $Ru^{2+/3+}$ couple was electrochemically reversible, and as illustrated in **Figure 5**, a clear ECL response was observed from the modified FTO electrodes in the presence of oxalate. This observation indicates that in the presence of lithium in the supporting electrolyte, the emission is not completely quenched by the semiconductor surface. The observation is particularly striking given that the excited state is most likely located on the dicarboxy-bpy ligand closest to the electrode. However, it is entirely consistent with the large ΔE_p observed in cyclic voltammetry at relatively slow scan rates, which indicates weak electronic coupling between the adsorbate and electrode.

An ECL response was generated at this monolayer using amino acids as the coreactant, and the intensity of the ECL signal depended on the identity and concentration of the amino acid. However, as expected on the basis of well-documented solution-phase measurements (33), the magnitude of this ECL signal varied significantly, with proline and hydroxy-proline being the

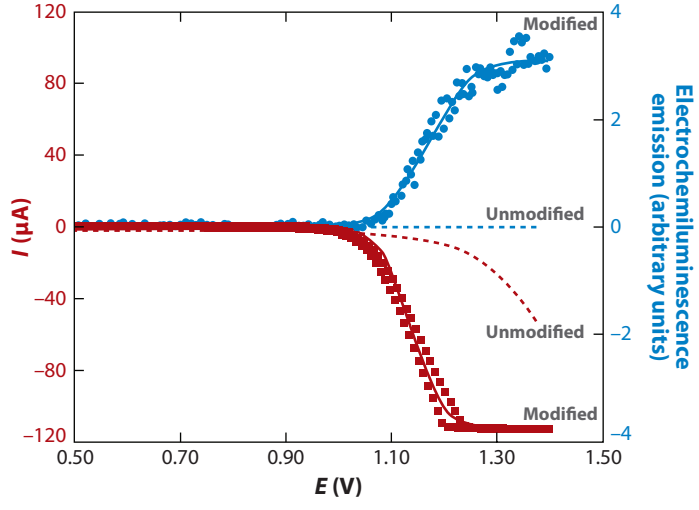

Figure 5

Potential dependence of current (*red*) and emission intensity (*blue*) of an unmodified (*dashed lines*) and modified (*solid lines*) electrode in 0.4 M Na_2SO_4 solution containing 10 mM $Na_2C_2O_4$ (pH 4.7). The scan rate is 100 mV s^{-1}, and the voltage sweep direction is from 0.5 to 1.4 V. Reprinted with permission from Reference 32.

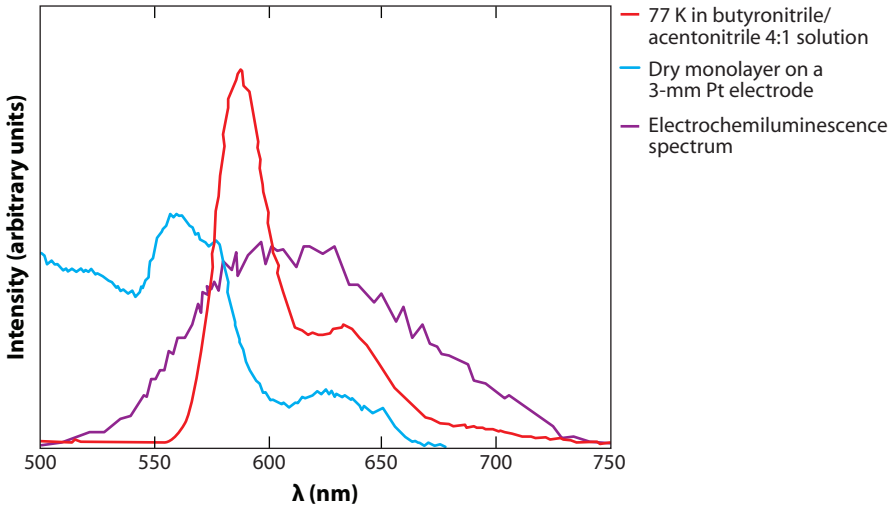

Figure 6

Emission spectra of a dry RuBpySH monolayer on a 3-mm Pt electrode, $\lambda_{exc} = 290$ nm. Emission spectra of RuBpySH at 77 K in butyronitrile/acetonitrile 4:1 solution. Electrochemiluminescence spectrum from an RuBpySH monolayer ($\Gamma = 5 \times 10^{-11}$ mol cm^{-2}) recorded following a potential step to 1.20 V. The solution contains 0.1 M $TBABF_4$ in acetonitrile and 0.1 M tripropylamine (TPA). Reprinted with permission from Reference 34. Abbreviations: RuBpySH, ruthenium 5,5′-bis(mercaptomethyl)-2,2′-bipyridine; $TBABF_4$, tetrabuthylammoniumtetrafluoroborate.

most efficient at generating ECL. The ECL intensity varied linearly over $0.2 \leq$ [proline] ≤ 1 nM, whereas for hydroxy-proline, the dynamic range was between 1 and 10 nM (32).

Other systems in which a metal complex is immobilized close to an electrode surface, yet still generates ECL, have been reported (34). Monolayers of $[Ru(bpy)_2(bpySH)](PF_6)_2$ (where bpySH refers to 5,5′-bis(mercaptomethyl)-2,2′-bipyridine) were formed on micro and macro platinum electrodes by spontaneous adsorption from micromolar solutions of the complex in 50:50 v/v water:acetone. The monolayers were reversibly switched between the Ru^{2+} and Ru^{3+} forms. As illustrated in **Figure 6**, dry monolayers display luminescence properties similar to those of powder samples of the complex, indicating that the monolayer has characteristics of the solid-state sample rather than the complex in solution. Significantly, there is weak adsorbate-electrode electronic communication that leads to a relatively low standard heterogeneous electron-transfer rate constant, k°, of $0.9 \pm 0.1 \times 10^4$ s^{-1}, and efficient ECL is generated using TPA as the coreactant.

The advantages of performing an assay at an interface, combined with the sensitivity and control of the ECL response, have been exploited in both nucleic acid and antigen assays. The general principles of ECL detection using this approach are outlined in **Figure 7**. Single-stranded DNA (ssDNA) is immobilized on the surface of the electrode (or substrate), then the complementary target strand of ssDNA tagged with the ECL label hybridizes with the immobilized ssDNA strand. The electrode assembly is placed in a solution or flow-cell containing a coreactant. ECL generation is then triggered by applying either a potential pulse or a sweep, and ECL is measured. For example, Miao & Bard (35) used $[Ru(bpy)_3]^{2+}$–type labels attached to a target/complementary ssDNA strand to detect DNA derived from *Bacillus anthracis*. The authors used TPA as the coreactant.

The determination of up- or downregulated proteins in biological samples ranging from whole blood to urine and saliva remains a powerful approach to diagnosing diseases from cardiovascular

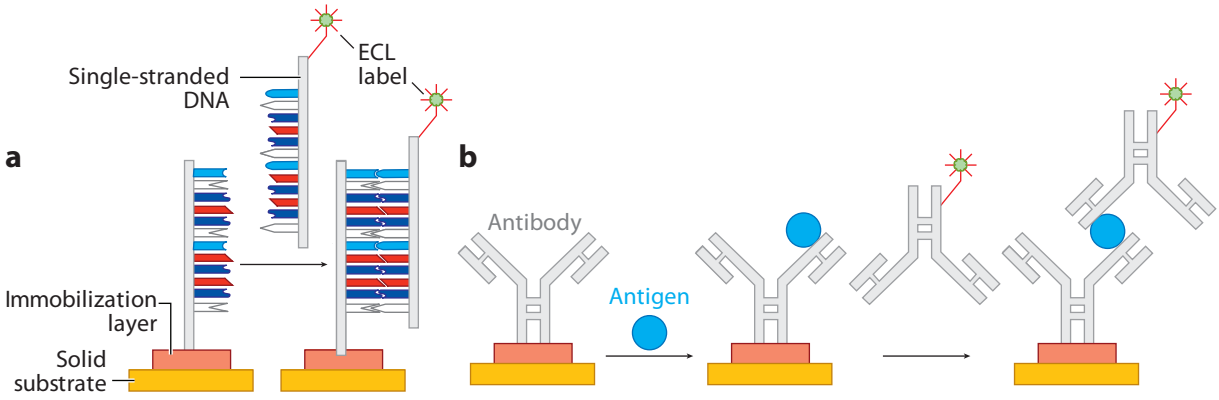

Figure 7

Schematic diagram of solid-state electrochemiluminescence (ECL): (*a*) detection of DNA hybridization and (*b*) sandwich-type immunoassay. Reprinted with permission from Reference 35.

disease to cancer. For example, C-reactive protein (CRP) in human serum may be useful as a marker of recent or ongoing myocardial infarction. However, as technology drives down limits of detection, CRP's value as an early marker of disease, and as a predictor of the onset of coronary events such as angina, is becoming increasingly clear. To determine CRP concentrations in human plasma and serum, Miao & Bard (35) immobilized biotynilated anti-CRP onto a Au(111) substrate that was previously coated with a layer of avidin covalently linked to a thiol monolayer. CRP and anti-CRP tagged with $[Ru(bpy)_3]^{2+}$ labels were conjugated to the surface layer, then the modified electrode was immersed in a TPA solution for ECL generation.

4.3. Polymer Films

Thin films can generate significantly higher ECL responses compared to monolayers, as they combine the advantages of immobilization demonstrated with two-dimensional monolayers with the higher ECL reagent available to them due to their three-dimensional nature. However, this advantage is only realized if the coreactant and ECL reagent are available throughout the film's thickness. Realizing this goal demands careful attention to the kinetics of ECL reagent generation, which involves heterogeneous electron transfer across the electrode/film interface as well as charge propagation through the film and the transport of coreactants throughout the layer. The size of a labeled biomolecule could lead to limitations in the transport of the analyte.

The ECL properties of the metallopolymer $[Ru(bpy)_2(PVP)_{10}]^{2+}$, where PVP is poly(4-vinylpyridine), have been studied in some detail predominantly through the use of oxalate, TPA, and other small molecules as coreactants (36). A key difference between conventional solution-phase luminescence experiments (both ECL and photoluminescence) and thin films is that the concentrations of luminophores are dramatically different: typically micromolar compared to molar concentrations within films. The high concentrations found in thin films may limit the overall luminescence efficiency, for instance by self-absorbance in light-stimulated emission. In the case of some ECL-generation schemes, self-quenching may be an issue because the emissive Ru^{2+*} state is created from reduction of electrogenerated Ru^{3+} by the target analyte. Rather than producing the desired light-emission process, Ru^{2+*} can be quenched by electron transfer to adjacent Ru^{3+} moieties that may be the dominant species within the film. For example, as shown in **Figure 8**, the emission intensity decreases by approximately 80% when 20% of a $[Ru(bpy)_2(PVP)_{10}]^{2+}$ film

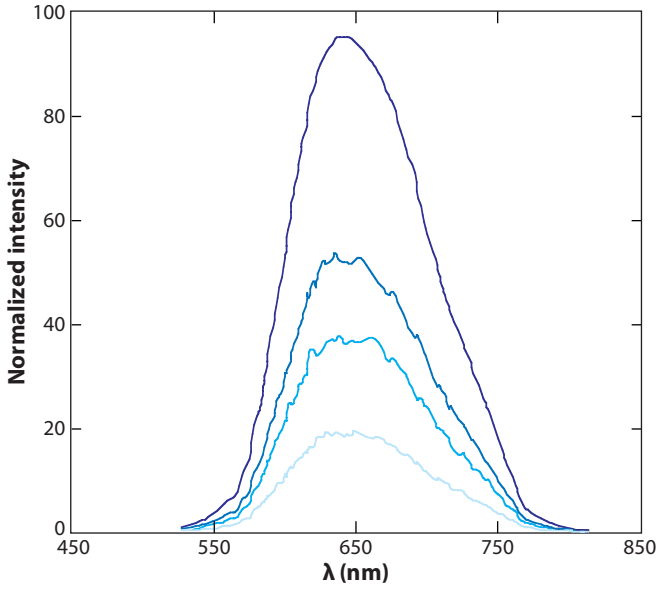

Figure 8

Effect of partially oxidizing an $[Ru(bpy)_2(PVP)_{10}]^{2+}(PF_6)_2$ film deposited on an indium tin oxide electrode in contact with an aqueous 0.1-M H_2SO_4 solution on the emission spectrum. (*Top to bottom*) The percentages of Ru^{3+} centers are 0, 6, 10, and 20. Reprinted with permission from Reference 36.

is oxidized (i.e., the loss of emission intensity greatly exceeds that expected on the basis of the reduced luminophore concentration due to the quenching effect of Ru^{3+}). Such effects most likely occur within ECL-generating systems, and a more intense response may be achieved by decreasing the loading of the ECL-generating reagent so as to minimize quenching effects. Surface immobilization may bring significant positive benefits. For example, the overall efficiency of the ECL reaction for the metallopolymer film is almost four times higher than that for $[Ru(bpy)_2(PVP)_{10}]^{2+}$ dissolved in solution.

Sensitive, selective detection of DNA is central to many clinical tests, pathogen detection, and other methods utilizing polymerase chain reaction, including genetic disease screening based on oligonucleotide hybridization and molecular genotoxicity studies. Electrochemistry provides simple, sensitive, and inexpensive approaches to detecting DNA hybridization and damage. One of the most sensitive approaches was first reported by Thorp et al. (37), who showed that $[Ru(bpy)_3]^{2+}$ oxidizes guanine bases in DNA and oligonucleotides in an electrochemical catalytic pathway. Direct ECL involving DNA has been demonstrated using the metallopolymer $[Ru(bpy)_2PVP_{10}](ClO_4)_2$ as the luminophore and guanine as the coreactant (38). In this scheme, ultrathin films (~10 nm) of the ECL-generating polymer were assembled layer by layer with DNA. A square-wave voltammetric waveform was applied to oxidize Ru^{2+} to Ru^{3+}, and ECL was measured. Significant ECL generation only occurred when guanine bases were present in the oligonucleotide films. The mechanism for light emission may involve the interaction of guanine radicals with Ru^{3+} to generate the Ru^{2+*} excited state or the reduction of Ru^{2+} to Ru^{+} by the guanine radicals, followed by annihilation of Ru^{3+} and Ru^{+}. Researchers have investigated the detection of DNA damage through this approach by changing the metal center from ruthenium to osmium (39). The redox potential of the osmium polypyridine centers is approximately 500 mV less positive than for ruthenium. Therefore, the osmium polymer does not generate ECL in the presence of guanine; however, as

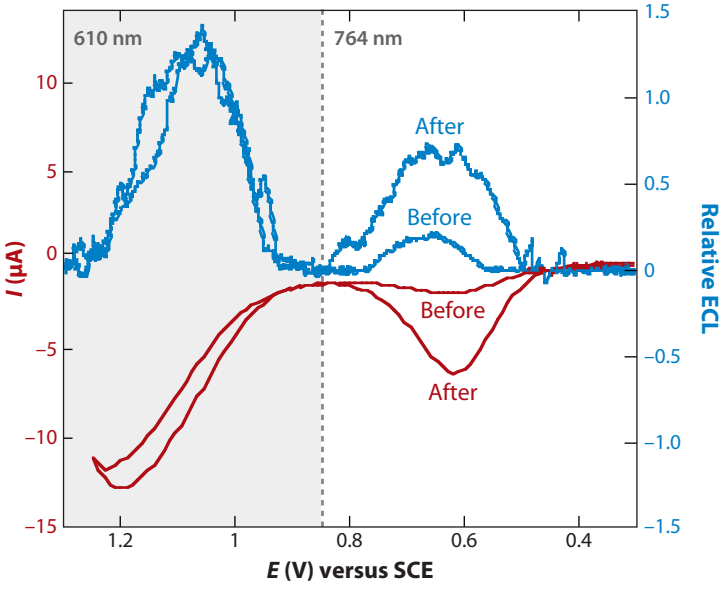

Figure 9

Square-wave voltammetry (SWV; *red*) and electrochemiluminescence (ECL; *blue*) for (Os-Ru/Poly G·Poly C)$_2$ films on pyrolitic graphite (PG) electrodes in pH-5.5 buffer before and after 20-min incubation at 37° C with Fenton's reagent. ECL emission is initially at ∼764 nm and switches to ∼610 nm at 0.8 V (*gray dashed line*). Reprinted with permission from Reference 39.

illustrated in **Figure 9**, because oxo-guanine is more easily oxidized than the parent, oxo-guanine can reduce electrogenerated Os^{3+} sites to produce electronically excited Os^{2+*} centers that emit at approximately 700 nm. The approach to detecting oxidative and chemical damage within DNA has also been extended to investigate oxo-adenine. Thin films combining DNA, $[Ru(bpy)_2(PVP)_{10}]^{2+}$, and $[Os(bpy)_2(PVP)_{10}]^{2+}$ reveal that Os^{2+} sites can selectively catalyze oxo-guanine and that the higher oxidizing power of the Ru^{2+} sites with a formal potential of approximately +1.1 V are capable of oxidizing both oxo-adenine and oxo-guanine. This multicomponent approach can also provide insight into strand cleavage, and it allows for the detection of both chemical and oxidative DNA damage.

Thin films of other polymers and composites have also been investigated. The objectives included increasing the total amount of luminophore immobilized and increasing the overall conductivity, thereby increasing the rate of luminophore production to engineer the photophysical properties of the excited state through plasmonic effects. For example, the electrochemistry and ECL of $[Ru(bpy)_3]^{2+}$/TPA ion exchanged in Eastman AQ–carbon nanotube (CNT) composite films were investigated via a glassy carbon working electrode (40). The sensor showed excellent stability over a period of two weeks with an essentially unchanged ECL response. The composite also showed high sensitivity, with a detection limit of 30 pM for TPA. It was proposed that because enzymes such as alcohol dehydrogenase can be incorporated into these films, such enzymes could provide a suitable matrix for ECL-based biosensors. The nature of the ECL reagent bound within polymers has recently been extended to iridium systems. For example, $[Ir(ppy)]_3$ and $[Ir(btp)_2(acac)]$ bound in polymer matrices display ECL upon application of positive potentials in the presence of TPA as a coreactant (41). $[Ir(ppy)]_3$ and $[Ir(btp)_2(acac)]$ display significant and reproducible ECL when bound in PVK [poly(3-3′(vinylcarbazole)] with no detectable signal in

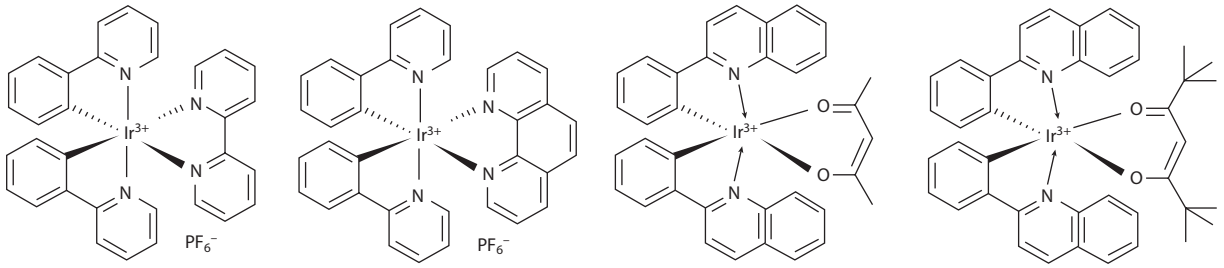

Figure 10

Metal complexes used in an electrochemiluminescence study (42). Reprinted with permission from Reference 42.

Nafion. The highest ECL in all systems resulted from luminophore/PVK in MeCN solution with Bu_4NPF_6 as the electrolyte.

Other monomeric systems that may lend themselves toward immobilization include orthometallated iridium(III) systems such as those illustrated in **Figure 10**. Very efficient ECL was measured upon tuning the excited states in by varying the ligands attached to the metal center (42). As illustrated in **Figure 11**, this tuning of the highest and lowest occupied molecular orbital levels (oxidation potential and reduction potential) of iridium(III) complexes resulted in a 77-fold increase in the ECL from iridium(III) complexes in the presence of TPA over the ECL from the $[Ru(bpy)_3]^{2+}$/TPA system.

Compared to iridium complex applications, application of osmium complexes for ECL production is somewhat limited due to larger spin-orbit coupling, which typically results in shorter excited-state lifetimes and weaker emission (43). However, the development of such sensors would be advantageous because osmium systems are more photostable than their ruthenium analogs, they

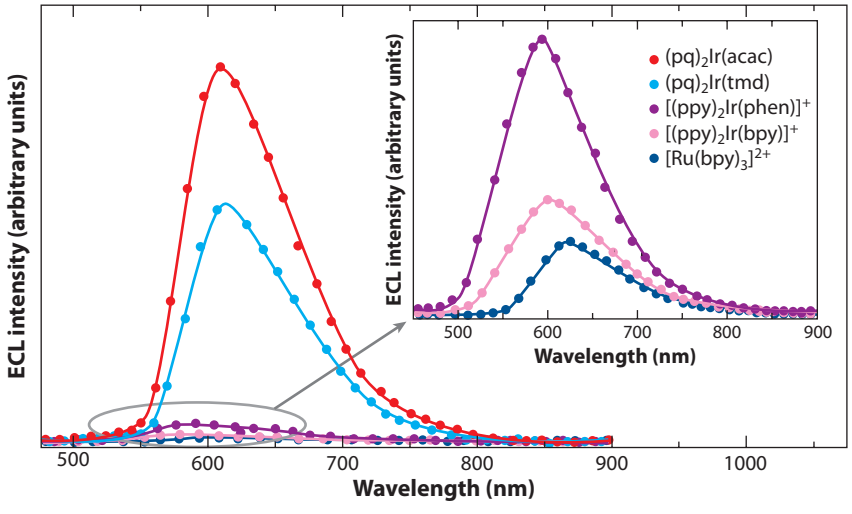

Figure 11

Electrochemiluminescence (ECL) spectra of $[Ru(bpy)_3]^{2+}$, $[(ppy)_2Ir(bpy)]^+$, $[(ppy)_2Ir(phen)]^+$, $(pq)_2Ir(acac)$, and $(pq)_2Ir(tmd)$ in acetonitrile solution. (*Inset*) Magnified ECL data for $[Ru(bpy)_3]^{2+}$, $[ppy_2Ir(bpy)]^+$, and $[ppy_2Ir(phen)]^+$. Reprinted with permission from Reference 42.

usually oxidize at less anodic potentials, and their longer emission wavelength may be more suitable for some applications (e.g., there may be less spectral overlap with the absorption spectrum of whole blood). Despite the issue of spin-orbit coupling, some osmium complexes exhibit a more intense ECL emission than does $[Ru(bpy)_3]^{2+}$. For example, $[Os(phen)_2(dppene)]^{2+}$ generates ECL in aqueous and mixed aqueous:MeCN solutions when TPA is used as the coreactant, and its ECL efficiency was twofold greater than that of $[Ru(bpy)_3]^{2+}$. The emission efficiency could be increased up to threefold in the presence of the nonionic surfactant Triton X-100 (44).

The ability to structure films on the nanoscale is an important goal for the production of devices and sensors. A novel procedure to incorporate tris(2-2′-bipyridyl)ruthenium(II) and $[Ru(bpy)_3]^{2+}$ into Nafion Langmuir–Schaefer films has been described (45, 46). Nafion Langmuir–Schaefer films with incorporated $[Ru(bpy)_3]^{2+}$ were fabricated via a one-step procedure that allowed the luminophore to be directly incorporated within the Langmuir monolayer during its formation. Direct ECL was then demonstrated for 6-nm Nafion films assembled using the Langmuir–Schaefer films.

5. PARTICLE-BASED SYSTEMS

5.1. Overview

Particles are well suited for assays because they can be easily multiplexed, offer a large surface area that can provide a larger signal (but not necessarily an improved signal-to-noise ratio), and may provide a greater availability for antibody/nucleic acid binding sites. For example, methods to detect DNA hybridization based on $[Ru(bpy)_3]^{2+}$-doped silicon nanoparticles (47) through use of a hybridization chip with electric field–aided mismatch discrimination have been reported (48).

ECL experiments have also been performed on dendritic complexes containing 2-, 4-, and 8-ruthenium units in both homogeneous and heterogeneous assay formats (23). With the use of nanoparticle technology (i.e., attaching the dendrimeric units to a paramagnetic bead that can then be magnetically attracted to the electrode), the ECL in these systems has been shown to increase linearly with the number of active ruthenium centers and to overcome the problems associated with the slow diffusion of multimetallic assemblies to the electrode surface. However, intense background signals due to nonspecific binding were observed in the dendrimer containing 8-ruthenium units; this interference lowered the final ECL intensity and sensitivity.

5.2. Metal Nanoparticles

An interesting method for immobilizing $[Ru(bpy)_3]^{2+}$ on electrode surfaces has been developed by Wang and coworkers (49). First, as illustrated in **Figure 12**, electrostatic interactions between citrate-capped gold nanoparticles (AuNPs) and $[Ru(bpy)_3]Cl_2$ in aqueous medium were used to fabricate $[Ru(bpy)_3]^{2+}$–AuNP aggregates (Ru–AuNPs). Then, Au–S interactions between the as-formed Ru–AuNPs and the sulfhydryl groups were used to immobilize the Ru–AuNPs on a sulfhydryl-derivitized indium tin oxide (ITO) electrode surface. Interestingly, the redox peak of the $Ru^{2+/3+}$ couple was not observed in cyclic voltammetry. However, fairly intense ECL was generated using TPA as a coreactant, which was stable for several scans.

Platinum–$[Ru(bpy)_3]^{2+}$ aggregates have also been produced and ECL generated by oxidizing the ruthenium centers in the presence of TPA (50). Platinum nanoparticles (PtNPs) were also incorporated into an Eastman AQ55D/ruthenium(II) tris(bipyridine) (PtNPs/AQ/$[Ru(bpy)_3]^{2+}$) colloidal material, and the ECL in a solid-state device was reported (51). The cation ion–exchanger AQ was used to immobilize $[Ru(bpy)_3]^{2+}$ and PtNPs as dispersant. Directly coating

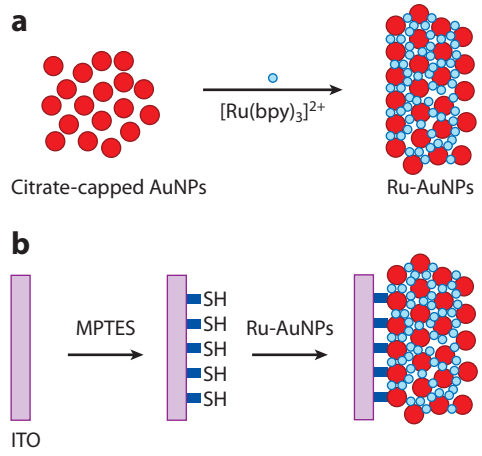

Figure 12

(*a*) Formation of Ru–AuNPs ($[Ru(bpy)_3]^{2+}$–gold nanoparticles) in aqueous medium due to electrostatic interactions between $[Ru(bpy)_3]^{2+}$ and citrate-capped AuNPs. (*b*) Immobilization of Ru–AuNPs on a sulfhydryl-derivatized indium tin oxide (ITO) electrode surface. Reprinted with permission from Reference 49. Abbreviation: MPTES, mercaptopropyltriethoxysilane.

PtNPs/AQ/$[Ru(bpy)_3]^{2+}$ on the surface of a glassy carbon electrode, followed by potential sweep in the presence of TPA, produces ECL with an impressive femtomolar limit of detection.

Multilayer films of Nafion-stabilized magnetic nanoparticles [Nafion/Fe_3O_4 (NSMNPs)] incorporating $[Ru(bpy)_3]^{2+}$ have been used to create a TPA-based sensor platform. The use of magnetic nanoparticles for immunomagnetic separations is well established (52), and as illustrated in **Figure 13**, these nanoparticles can be concentrated on a platinum electrode surface via an external magnet (53). This platform is more sensitive than are conventional thin films on electrodes, presumably due to the fast mass transport in the NSMNP films.

5.3. Silica Nanoparticles

Encapsulating ECL reagents may offer particular advantages including reduced interference through size/charge, enhanced sensitivity, and ability to introduce surface binding groups for biomolecules, wider dynamic range and enhanced stability. For example, ECL sensors have been developed in which $[Ru(bpy)_3]^{2+}$ was doped into the silica nanoparticles (illustrated in **Figure 14**) (54). The system had a detection limit of 2.8 nM for TPA, which was three orders of magnitude lower than that observed for Nafion-based systems. Moreover, the functionalized nanoparticles were stable for extended periods.

5.4. Carbon Nanotubes

Functionalizing electrodes with CNTs is an attractive option for electroanalysis because of their large surface area and their ability to efficiently transfer electrons, although the latter factor depends on their thermal and chemical history (55–63). Different strategies have been developed for immobilizing $[Ru(bpy)_3]^{2+}$ onto CNTs, mainly by forming CNT/polymer/$[Ru(bpy)_3]^{2+}$ composites (64, 65). Popular polymers include Nafion (45, 66–70) and Eastman-AQ55D polymers (72). An interesting approach recently reported by Li and coworkers (73) involved the use of partially sulfonated polystyrene with CNTs and $[Ru(bpy)_3]^{2+}$. This novel composite was tested for the ECL detection of TPA and 2-(dibutylamino)ethanol.

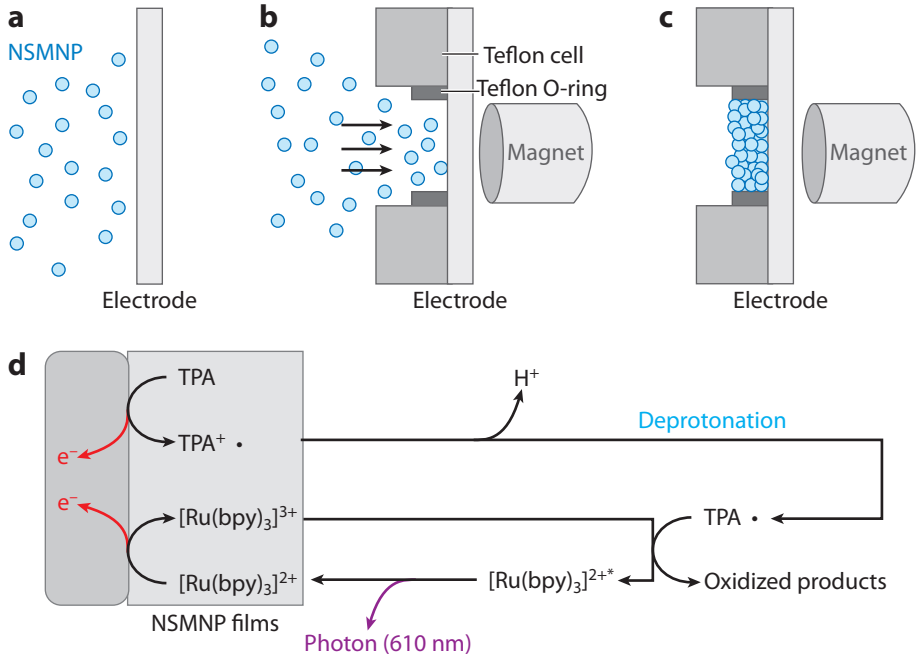

Figure 13

(*a–c*) Formation of a NSMNP (Nafion/Fe_3O_4 nanoparticle)-modified electrode. (*d*) Electrochemiluminescence from $[Ru(bpy)_3]^{2+}$ immobilized in the multilayer films on a platinum electrode surface in the presence of a coreactant, tripropylamine (TPA). Reprinted with permission from Reference 53.

As discussed above, the sensitive detection of DNA has been widely investigated because of its importance in clinical diagnosis. **Figure 15** illustrates an approach developed by Wang and coworkers (67) in which polymer/CNT composite films formed from solutions containing Nafion and multiwalled carbon nanotubes (MWNTs) were loaded by soaking in $[Ru(bpy)_3]^{2+}$ solutions. Significantly, this procedure allowed label-free detection of DNA based on the electrocatalytic

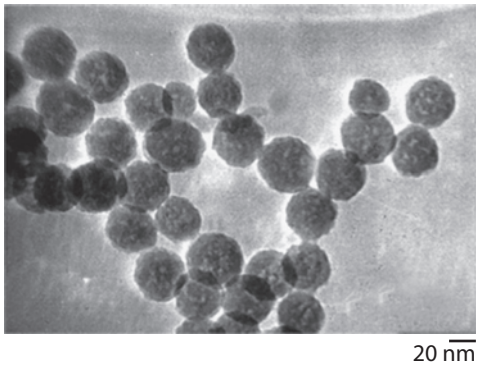

Figure 14

Transmission electron microscopy image of $[Ru(bpy)_3]^{2+}$-doped silica nanoparticles. Reprinted with permission from Reference 54.

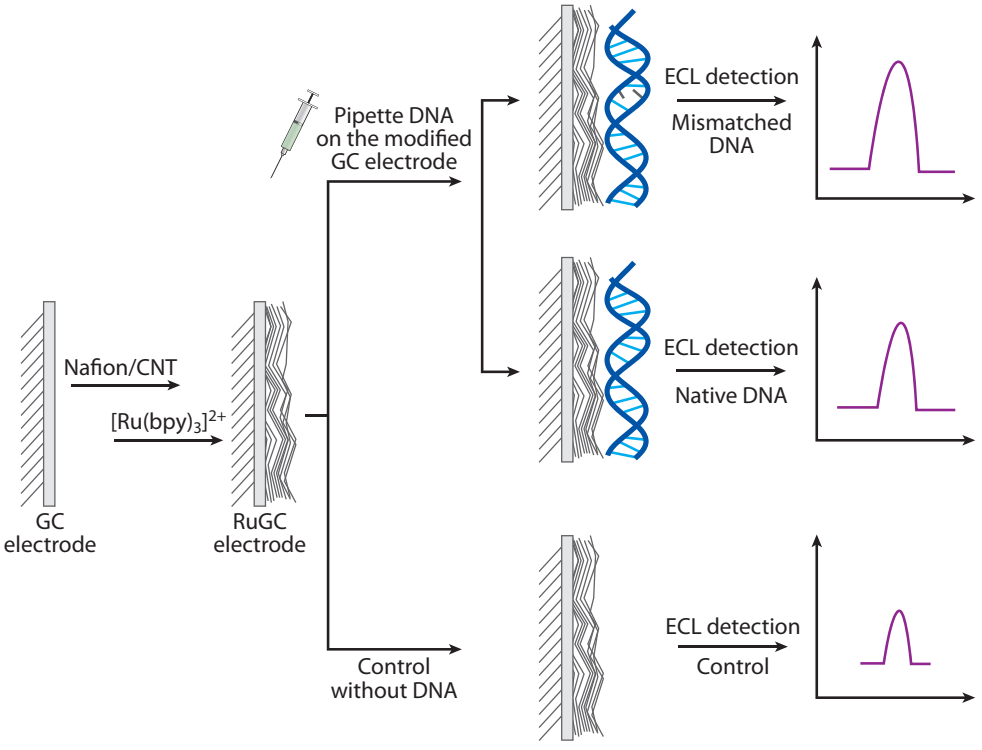

Figure 15

Schematic of the procedure employed for the modification of the glassy carbon (GC) electrode and electrochemiluminescence (ECL) detection. Abbreviation: CNT, carbon nanotube. Reprinted with permission from Reference 67.

detection of guanine and adenine bases. For instance, ECL signals were obtained for double-stranded DNA, allowing DNA from salmon testes to be detected at nanomolar concentrations.

Other important analytes of clinical relevance have been detected via ECL (74–77). For example, glucose was quantitatively detected by encapsulating glucose oxidase within a CNT/Nafion film–modified glassy carbon electrode (77). ECL were also used to detect the neurotransmitters dopamine and epinephrine by evaluating their inhibition effect on the ECL of Nafion/$[Ru(bpy)_3]^{2+}$ deposited on CNTs (78). This approach was shown to be highly sensitive (fractions of millimoles) and selective even in the presence of a 200-fold excess of ascorbic acid, which is known to be the most important interferant in neurotransmitter determination.

Figure 16 illustrates an interesting investigation by Wohlstadter and coworkers (79), who used single-walled nanotube (SWNT)–polyethylene vinylacetate (EVA)–$[Ru(bpy)_3]^{2+}$ for ECL detection of immunoassay for α-fetoprotein (AFP). In this study, a novel AFP immunoassay was developed by functionalizing streptavidin-coated nanotube-EVA composites with biotinylated anti-AFP. This SWNT/ EVA/$[Ru(bpy)_3]^{2+}$ system allowed AFP to be detected in the 0.1–100-nM range.

Beyond physical entrapment, the ECL reagent has been covalently linked to the CNT surface. This approach has the advantage of avoiding the leaching that often occurs when electrostatic binding is used and opens up the possibility of controlling the extent of electronic communication between the CNT and the luminophore by changing the bridging ligand structure. For

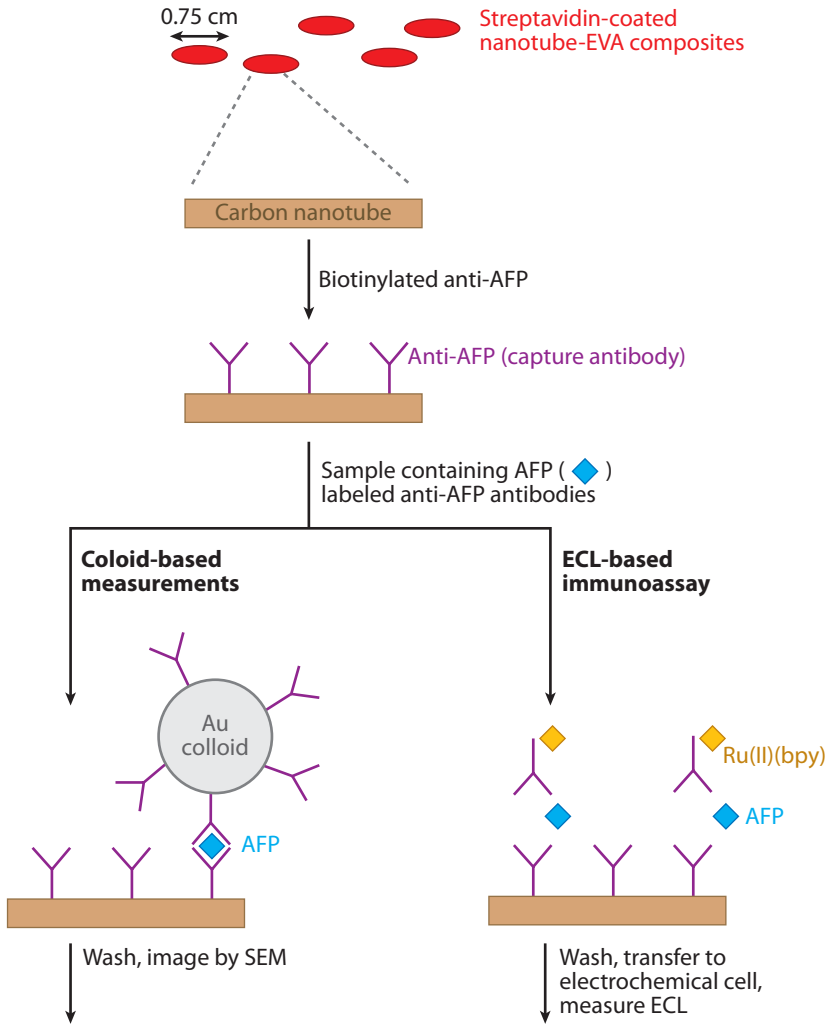

Figure 16

Schematic of the procedure employed for the fabrication of an electrochemiluminescence (ECL) immunosensor for detection of an α-fetoprotein (AFP). Abbreviations: EVA, polyethylene vinylacetate; SEM, scanning electron microscopy. Reprinted with permission from Reference 79.

example, Tao and coworkers (80) produced carboxy-terminated MWNTs by treating them with concentrated nitric acid. The carboxyl groups were then activated with succinimide and carbodiimide derivates. The ECL reagent, $[Ru(bpy)_2(5\text{-amino-}1,10\ \text{phenanthroline})]^{2+}$, was then bound by means of an amide or peptide bond. The system showed good sensitivity and allowed detection of micromolar concentrations of TPA.

5.5. Quantum Dots

Semiconductor nanocrystals (NCs) and quantum dots (QDs) have received considerable interest because of their outstanding luminescent properties, and they have been applied in many areas of

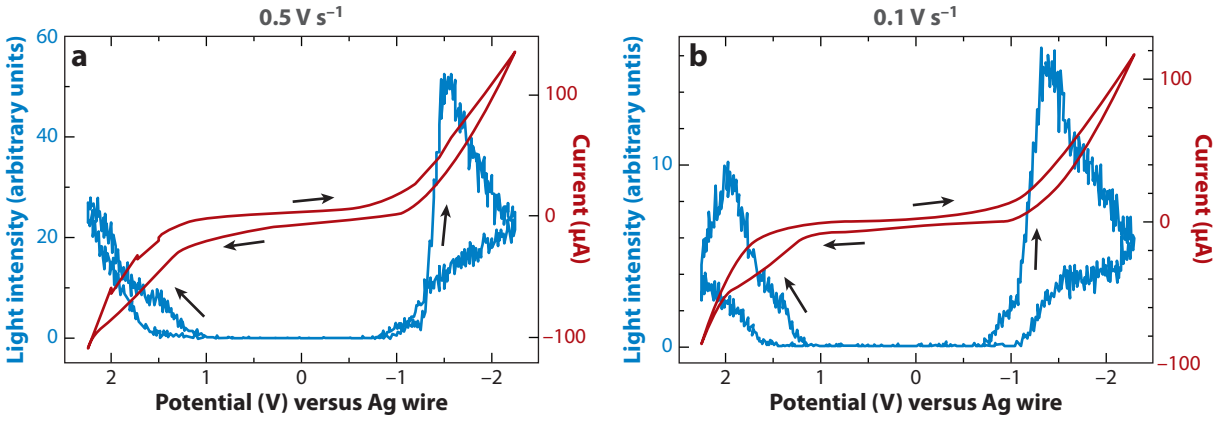

Figure 17

Cyclic voltammetry and electrochemiluminescence curves of CdSe nanocrystals in 0.1 M tetrabuthylammonium perchlorate (TBAP) in dichloroethane at different scan rates. Reprinted with permission from Reference 85.

fundamental importance (81–83). ECL reports from NCs are scarce because of their low solubility and the low stability of their oxidized and reduced forms (84). However, Bard and coworkers (85–89) recently demonstrated that QDs are electrically excitable in both nonaqueous (85–87) and aqueous media (88, 89). For example, CdSe NCs were synthesized in dichloroethane using the method developed by Aldana and coworkers (90). Typical cyclic voltammetry and ECL of CdSe NCs in dichloroethane are illustrated in **Figure 17**.

NCs can be oxidized or reduced during the potential cycling based on the following reactions (89):

$$R^{\cdot -} + R^{\cdot +} \rightarrow R^{*} + R \tag{10}$$

and

$$R^{*} \rightarrow R + h\nu. \tag{11}$$

ECL occurs when the electrogenerated reduced species, $R^{\cdot -}$, collides with the oxidized form, $R^{\cdot +}$, producing R^{*} via an annihilation process.

Liu and coworkers (91) synthesized water-soluble mercaptopropionic acid–protected CdTe NCs for ECL detection of catecol derivatives. Stable and intense anodic ECL was obtained at approximately 1.2 V versus Ag/AgCl in phosphate buffer (pH 9.3). The ECL emission involved the generation of superoxide ions at the ITO electrode surface, which injected an electron into CdTe to form a CdTe anion. The collision between this anion and the oxidation product led to the formation of an excited-state species that emits light at ~580 nm. The detection of catecols was achieved by measuring the quenching of the ECL emission by the electrooxidized products of catecols, dopamine, and L-adrenaline. Interestingly, common interferences such as uric acid and ascorbic acid were found to quench the anodic ECL emission very weakly. The emission wavelength depends on the band gap of QDs, which is influenced by their size (92). It has also been demonstrated that this quenching mechanism is an ECL energy-transfer process, rather than a charge-transfer process.

Mercaptocarboxylic acid (MCA)-capped CdTe NCs were also synthesized for the ECL determination of H_2O_2 in aqueous solutions (93). MCA-capped CdTe NCs were prepared via a procedure described by Zhang and coworkers (94). The ECL emission was linear with H_2O_2 concentration in the range of 0.2–10 μM and detection limit of 0.06 μM (95). The ECL spectrum of

MCA-capped CdTe NCs exhibited a peak at ~620 nm, which was redshifted by approximately 50 nm with respect to the photoluminescence peak, suggesting that surface states played an important role in the ECL process (95).

Thioglycolic acid (TGA)-protected CdSe QDs were also used for the ECL detection of thiols (96). It is believed that the intermediate $OH^{\bullet}$ radical is the key species for producing holes-injected QDs. Thiol compounds have been used as model molecules to annihilate the $OH^{\bullet}$ radical and to investigate the effects of quenching on ECL emission. The thiols used were γ-*L*-glutamyl-*L*-cysteine-glycine, glutathione, and *L*-cysteine, which are known to be involved in many biological processes (97). The procedure achieved high sensitivity, suggesting that this novel method could be used for the simultaneous detection of both scavengers and generators of hydroxyl radicals in clinical tests.

Recently, ECL detection coupled with an enzymatic reaction was investigated (95). For the first time, the intrinsic ECL of CdSe QDs was coupled to the functioning of an oxidase enzyme [glucose oxidase (GOX)]. TGA-protected CdSe QDs were coimmobilized with GOX, and glucose was detected by measuring the decrease of the ECL response of the GOX-QDs after addition of glucose. This system demonstrated good stability, sensitivity, and reproducibility for the detection of glucose. This concept could also be extended to other classes of oxidase enzymes. An ECL immunosensor for detection of human immunoglobulin G (IgG) based on the combination of CdSe NCs/MWNTs with chitosan/3-aminopropryl-triethoxysilane (APS) has also been reported (98). Because APS has reactive amine groups, it can be used as an efficient cross-linker for the conjugation of biomolecules, for example for antibody immobilization. The results revealed that the addition of a coreactant such as $K_2S_2O_8$ was necessary to enhance the ECL signal, whereas APS catalyzed the reaction of CdSe NCs with $K_2S_2O_8$ based on the following mechanism:

$$\text{CdSe NCs} + ne^- \rightarrow n\text{CdSe}^{-\cdot}, \tag{12}$$

$$S_2O_8^{2-} + RC_3H_7 \rightarrow NH_2 \rightarrow SO_4^{2-} + SO_4^{-\cdot} + RC_3H_7 \rightarrow NH_2^{+\cdot}, \tag{13}$$

$$\text{CdSe}^{-\cdot} + SO_4^{-\cdot} \rightarrow \text{CdSe}^{*} + SO_4^{2-}, \tag{14}$$

and

$$\text{CdSe}^{*} \rightarrow \text{CdSe} + h\nu. \tag{15}$$

The detection of IgG using this ECL method yielded values that agreed well with those obtained from an ELISA (enzyme-linked immunosorbent assay) method.

An ECL-detection method based on mercaptoacetic acid-(RSH)-protected CdS QDs with cysteamine and AuNPs for detection of low-density lipoproteins (LDLs) using $S_2O_8^{2-}$ as coreactant has been reported (99). The schematic for the fabrication of the biosensor is illustrated in **Figure 18**. This system detected LDLs by measuring the decrease of the ECL signal resulting from the specific binding of LDLs with a ligand of LDL receptor (apoB100). Typical ECL profiles for LDLs are illustrated in **Figure 19**.

Very recently, ECL detection using organic nanoparticles has been demonstrated. Barbara and coworkers demonstrated the ECL detection of TPA from single immobilized nanoparticles made from a polyfluorene derivative (100) through use of a novel single-molecule spectroelectrochemistry technique (**Figure 20**) (101, 102). Significantly, the authors reported for the first time the exploration of the ECL behavior at the single-particle level, thus facilitating key investigations into the effects of particle heterogeneity on the ECL response. ECL has also recently been used for the observation of single-particle collisions. Fan & Bard (103) utilized ECL for single-particle collisions at PtNPs. A single event is characterized by the enhancement of the ECL during the collision of a PtNP on an ITO electrode, with concomitant catalysis and oxidation of $[Ru(bpy)_3]^{2+}$.

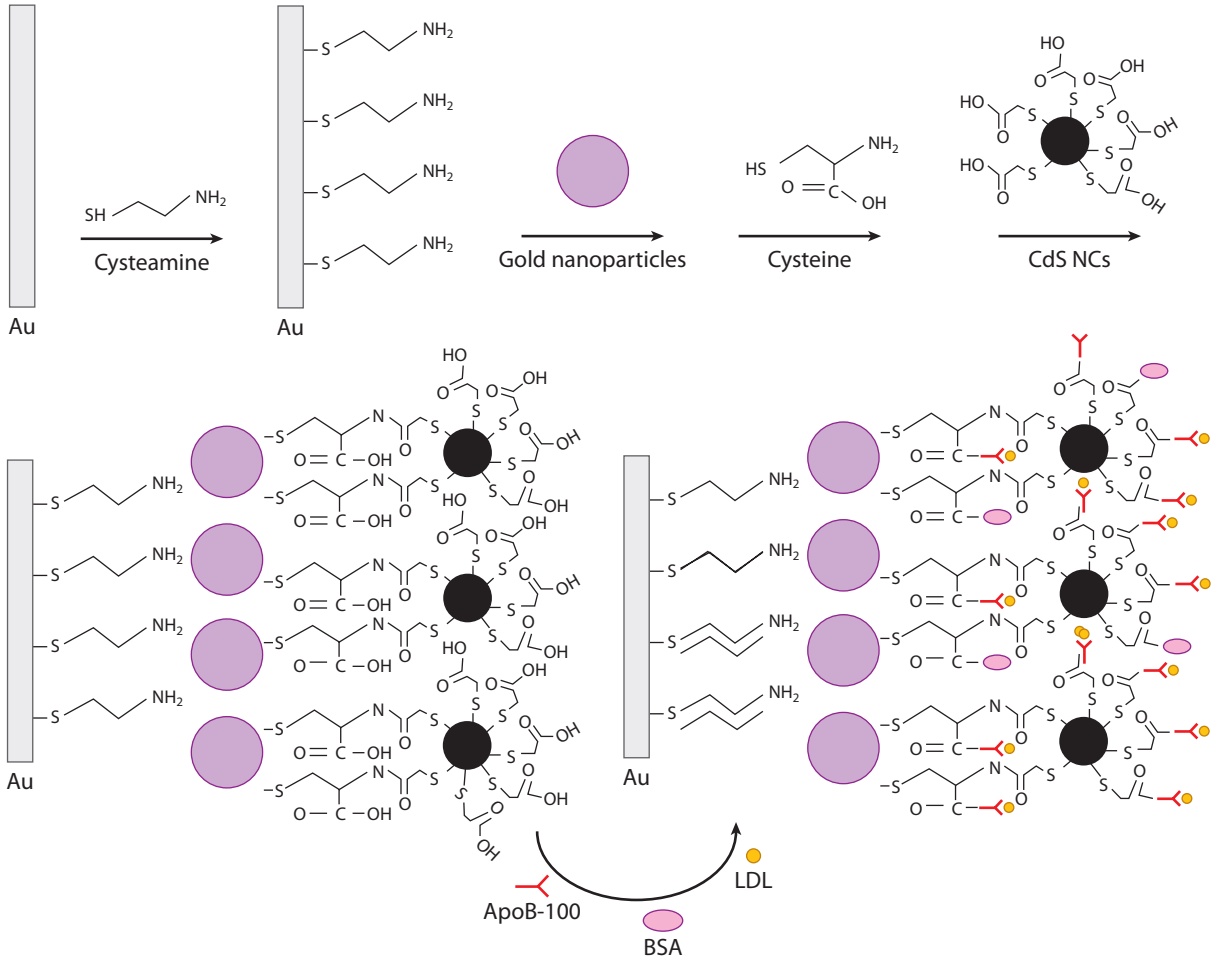

Figure 18

Schematic of the procedure employed for the functionalization of a Au electrode with Au and CdS nanoparticles for electrochemiluminescence detection of low-density lipoprotein (LDL) cholesterol. Abbreviations: BSA, bovine serum albumin; NCs, nanocrystals. Reprinted with permission from Reference 99.

Every collision produced a photon spike whose frequency and amplitude depended on the size and concentration of PtNPs.

6. PROSPECTIVE

Coreactant ECL is currently being used in a wide range of analytical applications including chromatography, clinical diagnostics, environmental projects (such as food and water testing), and biodefense (i.e., biowarfare agent detection). Currently, nearly 100 assays for biomarkers are available, including those for thyroid diseases, tumor and cardiac markers, cancer research, cell-signaling pathways, nucleic acids, fertility therapies, immunogenicity assays, and analytes relevant to infectious diseases. Tests for tumor markers, fertility hormones, thyroid function, cardiac, hepatitis, bone markers, Alzheimer's disease, anemia, diabetes, infectious diseases, AFP,

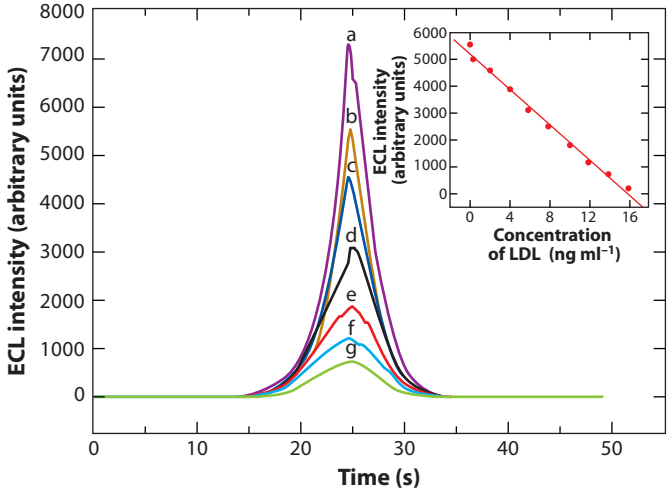

Figure 19

Electrochemiluminescence (ECL) curves obtained at different low-density protein (LDL) cholesterol concentrations (in nanograms per milliliter): (*a*) 0, (*b*) 0.025, (*c*) 2, (*d*) 6, (*e*) 10, (*f*) 12, and (*g*) 14. Scan rate, 100 mV s^{-1}. Reprinted with permission from Reference 99.

carcinoembryonic antigen, prostate-specific antigen, cancer markers, cytokeratin, anti–Borna disease antibodies, interleukin, and des-α-carboxy prothrombin are areas of active research and development. ECL will play an increasingly important role in these and other areas, especially in the development of portable, high-sensitivity devices such as biomedical point-of-care devices and field instruments for use in environmental research. Many of these applications will rely on the simplicity of the instrumentation, its small physical footprint, and its high sensitivity and selectivity. These advances will be driven by advanced materials, especially interfacial films and nanoparticle coatings, advances in microfluidics leading to total analytical or lab-on-a-chip systems, and new theoretical insights into the differences between plasmonic and quenching effects observed through optical and electrochemical excitation.

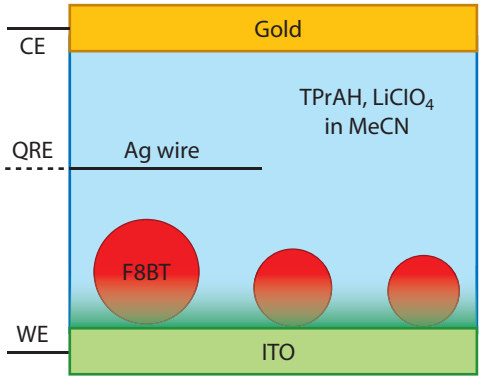

Figure 20

Schematic of the single-molecule spectroelectrochemistry cell. Abbreviations: CE, counter electrode; F8BT, polyfluorene derivative; ITO, indium tin oxide; QRE, quasi-reversible electrode; WE, working electrode. Reprinted with permission from Reference 102.

DISCLOSURE STATEMENT

The authors are not aware of any affiliations, memberships, funding, or financial holdings that might be perceived as affecting the objectivity of this review.

LITERATURE CITED

1. Visco R, Chandross E. 1964. Electroluminescence in solutions of aromatic hydrocarbons. *J. Am. Chem. Soc.* 86:5350–51
2. Santhanam K, Bard AJ. 1965. Chemiluminescence of electrogenerated 9,10-diphenylanthracene anion radical. *J. Am. Chem. Soc.* 87:139–40
3. Tokel-Takvoryan N, Hemingway R, Bard AJ. 1973. Electrogenerated chemiluminescence. XIII. Electrochemical and electrogenerated chemiluminescence studies of ruthenium chelates. *J. Am. Chem. Soc.* 95:6582–89
4. Pyati R, Richter M. 2007. ECL—electrochemical luminescence. *Annu. Rep. Prog. Chem., Sect. C: Phys. Chem.* 103:12–78
5. Miao W. 2008. Electrogenerated chemiluminescence and its related applications. *Chem. Rev.* 108:2506–53
6. Richter M. 2004. Electrochemiluminescence (ECL). *Chem. Rev.* 104:3003–36
7. Bard AJ, Debad J, Leland J, Sigal G, Wilbur J, Wohlstadter J. 2000. Chemiluminescence, electrogenerated. In *Encyclopedia of Analytical Chemistry: Applications, Theory, and Instrumentation*, vol. 11, ed. RA Meyers, p. 9842. Chichester: Wiley
8. Aboul-Enein H, Stefan R, van Staden J, Zhang X, Garcia-Campana A, Baeyens W. 2000. Recent developments and applications of chemiluminescence sensors. *Crit. Rev. Anal. Chem.* 30:271–89
9. Knight A. 2001. Electrogenerated chemiluminescence. *Chemiluminescence in Analytical Chemistry*, ed. A Garcia-Campana, W Baeyens, pp. 211–47. New York: Marcel Dekker
10. Richter M. 2002. Electrochemiluminescence. In *Optical Biosensors: Present and Future*, ed. FS Ligler, CA Rowe-Taitt, pp. 173–205. New York: Elsevier
11. Bard AJ. 2004. Miscellaneous topics and conclusions. In *Electrogenerated Chemiluminescence*, ed. AJ Bard, pp. 523–33. New York: Marcel Dekker
12. Gorman B, Francis P, Barnett N. 2006. Tris(2,2′-bipyridyl)ruthenium(II) chemiluminescence. *Analyst* 131:616–39
13. Glass R, Faulkner LR. 1981. Electrogenerated chemiluminescence from the tris(2,2′-bipyridine)ruthenium(II) system. An example of S-route behavior. *J. Phys. Chem.* 85:1160–65
14. Noffsinger J, Danielson N. 1987. Generation of chemiluminescence upon reaction of aliphatic amines with tris(2,2′-bipyridine)ruthenium(III). *Anal. Chem.* 59:865–68
15. Miao W, Choi J, Bard AJ. 2002. Electrogenerated chemiluminescence 69: the tris(2,2′-bipyridine)ruthenium(II), $(Ru(bpy)_3^{2+})$/tri-n-propylamine (TPrA) system revisited: a new route involving $TPrA^+$ cation radicals. *J. Am. Chem. Soc.* 124:14478–85
16. Wightman R, Forry S, Maus R, Badoco D, Pastore P. 2004. Rate-determining step in the electrogenerated chemiluminescence from tertiary amines with tris(2,2′-bipyridyl)ruthenium(II). *J. Phys. Chem. B* 108:19119–25
17. Pastore P, Badocco D, Zanon F. 2006. Influence of nature, concentration and pH of buffer acid-base system on rate determining step of the electrochemiluminescence of $Ru(bpy)_3^{2+}$ with tertiary aliphatic amines. *Electrochim. Acta* 51:5394–401
18. Kapturkiewicz A. 2004. Electron transfer and spin up–conversion processes. In *Electrogenerated Chemiluminescence*, ed. AJ Bard, pp. 163–212. New York: Marcel Dekker
19. Kanoufi F, Bard AJ. 1999. Electrogenerated chemiluminescence. 65. An investigation of the oxidation of oxalate by tris(polypyridine) ruthenium complexes and the effect of the electrochemical steps on the emission intensity. *J. Phys. Chem. B* 103:10469–80
20. Zhou M, Robertson G, Roovers J. 2005. Comparative study of ruthenium(II) tris(bipyridine) derivatives for electrochemiluminescence application. *Inorg. Chem.* 44:8317–25

21. Brooks S, Vinyard D, Richter M. 2006. Electrogenerated chemiluminescence of (bis-bipyridyl)ruthenium(II) acetylacetonate complexes. *Inorg. Chim. Acta* 359:4635–38
22. Richter M, Bard AJ, Kim W, Schmehl R. 1998. Electrogenerated chemiluminescence. 62. Enhanced ECL in bimetallic assemblies with ligands that bridge isolated chromophores. *Anal. Chem.* 70:310–18
23. Staffilani M, Hoss E, Giesen U, Schneider E, Harti F, et al. 2003. Multimetallic ruthenium(II) complexes as electrochemiluminescent labels. *Inorg. Chem.* 42:7789–98
24. Zhou M, Roovers J. 2001. Dendritic supramolecular assembly with multiple Ru(II) tris(bipyridine) units at the periphery: synthesis, spectroscopic, and electrochemical study. *Macromolecules* 34:244–52
25. Zhou M, Roovers J, Robertson G, Grover C. 2003. Multilabeling biomolecules at a single site. 1. Synthesis and characterization of a dendritic label for electrochemiluminescence assays. *Anal. Chem.* 75:6708–17
26. Zu Y, Bard AJ. 2000. Electrogenerated chemiluminescence. 66. The role of direct coreactant oxidation in the ruthenium tris(2,2′)bipyridyl/tripropylamine system and the effect of halide ions on the emission intensity. *Anal. Chem.* 72:3223–32
27. Zheng H, Zu Y. 2005. Emission of tris(2,2'-bipyridine)ruthenium(II) by coreactant electrogenerated chemiluminescence: from O_2-insensitive to highly O_2-sensitive. *J. Phys. Chem. B* 109:12049–53
28. Zu Y, Bard AJ. 2001. Electrogenerated chemiluminescence. 67. Dependence of light emission of the tris(2,2′)bipyridylruthenium(II)/tripropylamine system on electrode surface hydrophobicity. *Anal. Chem.* 73:3960–64
29. Workman S, Richter M. 2000. The effects of nonionic surfactants on the tris(2,2′-bipyridyl)ruthenium(II)-tripropylamine electrochemiluminescence system. *Anal. Chem.* 72:5556–61
30. Factor B, Muegge B, Workman S, Bolton E, Bos J, Richter M. 2001. Surfactant chain length effects on the light emission of tris(2,2′-bipyridyl)ruthenium(II)/tripropylamine electrogenerated chemiluminescence. *Anal. Chem.* 73:4621–24
31. Li F, Zu Y. 2004. Effect of nonionic fluorosurfactant on the electrogenerated chemiluminescence of the tris(2,2′-bipyridine)ruthenium(II)/tri-n-propylamine system: lower oxidation potential and higher emission intensity. *Anal. Chem.* 76:1768–72
32. Dennany L, O'Reilly E, Forster RJ. 2006. Electrochemiluminescent monolayers on metal oxide electrodes: detection of amino acids. *Electrochem. Commun.* 8:1588
33. Lee W, Nieman T. 1995. Evaluation of use of tris(2,2′-bipyridyl)ruthenium(III) as a chemiluminescent reagent for quantification in flowing streams. *Anal. Chem.* 67:1789–96
34. Bertoncello P, Pikramenou Z, Unwin P, Forster RJ. 2006. Adsorption dynamics and electrochemical and photophysical properties of thiolated ruthenium 2,2′-bipyridine monolayers. *J. Phys. Chem.* 110:10063–69
35. Miao W, Bard AJ. 2003. Electrogenerated chemiluminescence. 72. Determination of immobilized DNA and C-reactive protein on Au(111) electrodes using tris(2,2′-bipyridyl)ruthenium(II) labels. *Anal. Chem.* 75:5825–34
36. Dennany L, Hogan C, Keyes T, Forster RJ. 2006. Effect of surface immobilization on the electrochemiluminescence of ruthenium-containing metallopolymers. *Anal. Chem.* 78:1412–17
37. Johnston D, Glasgow K, Thorp H. 1995. Electrochemical measurement of the solvent accessibility of nucleobases using electron transfer between DNA and metal complexes. *J. Am. Chem. Soc.* 177:8933–38
38. Dennany L, Forster RJ, Rusling J. 2003. Simultaneous direct electrochemiluminescence and catalytic voltammetry detection of DNA in ultrathin films. *J. Am. Chem. Soc.* 125:5213–18
39. Dennany L, Forster RJ, White B, Smyth M, Rusling J. 2004. Direct electrochemiluminescence detection of oxidized DNA in ultrathin films containing $[Os(bpy)_2(PVP)_{10}]^{2+}$. *J. Am. Chem. Soc.* 126:8835–41
40. Zhang L, Guo Z, Xu Z, Dong S. 2006. Highly sensitive electrogenerated chemiluminescence produced at $Ru(bpy)_3^{2+}$ in Eastman–AQ55D–carbon nanotube composite film electrode. *J. Electroanal. Chem.* 592:63–67
41. Muegge B, Richter M. 2005. Electrogenerated chemiluminescence from polymer-bound ortho-metallated iridium(III) systems. *Luminescence* 20:76–80
42. Kim J, Shin I, Kim H, Lee J. 2005. Efficient electrogenerated chemiluminescence from cyclometalated iridium(III) complexes. *J. Am. Chem. Soc.* 127:1614–15

43. Creutz C, Chou M, Netzel T, Okumara M, Sutin N. 1980. Lifetimes, spectra, and quenching of the excited states of polypyridine complexes of iron(II), ruthenium(II), and osmium(II). *J. Am. Chem. Soc.* 102:1309
44. Walworth J, Brewer K, Richter M. 2004. Enhanced electrochemiluminescence from $Os(phen)_2(dppene)^{2+}$ (phen=1,10-phenanthroline and dppene=bis (diphenylphosphino)ethene) in the presence of Triton X-100 (polyethylene glycol tert-octylphenyl ether). *Anal. Chim. Acta* 503:241–45
45. Bertoncello P, Dennany L, Forster RJ, Unwin P. 2007. Nafion-tris(2-2′-bipyridyl)ruthenium(II) ultrathin Langmuir-Schaefer films: redox catalysis and electrochemiluminescent properties. *Anal. Chem.* 79:7549–53
46. Bertoncello P, Wilson N, Unwin P. 2007. One-step formation of chemically functionalized redox-active Langmuir-Schaefer Nafion films. *Soft Matter* 3:1300–7
47. Chang Z, Zhou J, Zhao K, Zhu N, He P, Fang Y. 2006. $Ru(bpy)_3^{2+}$-doped silica nanoparticle DNA probe for the electrogenerated chemiluminescence detection of DNA hybridization. *Electrochim. Acta* 52:575–80
48. Spehar-Deleze A, Schmidt L, Neier R, Kulmala S, de Rooij N, Koudelka-Hep M. 2006. Electrochemiluminescent hybridization chip with electric field aided mismatch discrimination. *Biosens. Bioelectron.* 22:722–29
49. Sun X, Du Y, Dong S, Wang E. 2005. Method for effective immobilization of $Ru(bpy)_3^{2+}$ on an electrode surface for solid-state electrochemiluminescene detection. *Anal. Chem.* 77:8166–69
50. Sun X, Zhang L, Dong S, Wang E. 2006. Pt nanoparticles: heat treatment–based preparation and $Ru(bpy)_3^{2+}$-mediated formation of aggregates that can form stable films on bare solid electrode surfaces for solid-state electrochemiluminescence detection. *Anal. Chem.* 78:6674–77
51. Du Y, Qi B, Yang X, Wang E. 2006. Synthesis of PtNPs/AQ/$Ru(bpy)_3^{2+}$ colloid and its application as a sensitive solid-state electrochemiluminescence sensor material. *J. Phys. Chem. B* 110:21662–66
52. Bruno J. 1998. In *Recent Research Developments in Microbiology*, vol. 1, ed. SG Pandalai, p. 25. Kerala, India: Trivandrum
53. Kim D, Lyu Y, Choi H, Min I, Lee W. 2005. Nafion-stabilized magnetic nanoparticles (Fe_3O_4) for $[Ru(bpy)_3^{2+}$ (bpy=bipyridine) electrogenerated chemiluminescence sensor. *Chem. Commun.* 2005:2966–68
54. Zhang L, Dong S. 2006. Electrogenerated chemiluminescence sensors using $Ru(bpy)_3^{2+}$ doped in silica nanoparticles. *Anal. Chem.* 78:5119–23
55. Agui L, Yanez-Sedeno P, Pingarron J. 2008. Role of carbon nanotubes in electroanalytical chemistry: a review. *Anal. Chim. Acta* 622:11–47
56. Valentini F, Palleschi G. 2008. Nanomaterials and analytical chemistry. *Anal. Lett.* 41:479–520
57. Hu X, Dong S. 2008. Metal nanomaterials and carbon nanotubes synthesis, functionalization and potential applications towards electrochemistry. *J. Mater. Chem.* 18:1279–95
58. Rivas G, Rubianes M, Rodriguez M, Ferreyra N, Luque G, et al. 2007. Carbon nanotubes for electrochemical biosensing. *Talanta* 74:291–307
59. Kim S, Rusling J, Papadimitrakopoulos F. 2007. Carbon nanotubes for electronic and electrochemical detection of biomolecules. *Adv. Mater.* 19:3214–28
60. Yang W, Thordarson P, Gooding J, Ringer S, Braet F. 2007. Carbon nanotubes for biological and biomedical applications. *Nanotechnology* 18:412001
61. Gong K, Yan Y, Zhang M, Su L, Xiong S, et al. 2005. Electrochemistry and electroanalytical applications of carbon nanotubes: a review. *Anal. Sci.* 21:1383–93
62. Gooding J. 2005. Nanostructuring electrodes with carbon nanotubes: a review on electrochemistry and applications for sensing. *Electrochim. Acta* 50:3049–60
63. Wang J. 2005. Carbon-nanotube based electrochemical biosensors: a review. *Electroanalysis* 17:7–14
64. Wang J, Musameh M, Lin Y. 2003. Solubilization of carbon nanotubes by Nafion toward the preparation of amperometric biosensor. *J. Am. Chem. Soc.* 125:2408–9
65. Wang J, Musameh M. 2003. Carbon nanotube/Teflon composite electrochemical sensors and biosensors. *Anal. Chem.* 75:2075–79

66. Pan W, Chen X, Guo M, Huang Y, Yao S. 2007. A novel amperometric sensor for the detection of difenidol hydrochloride based on the modification of $Ru(bpy)_3^{2+}$ on a glassy carbon electrode. *Talanta* 73:651–55
67. Wei H, Du Y, Kang J, Wang E. 2007. Label free electrochemiluminescence protocol for sensitive DNA detection with a tris(2,2′-bipyridyl)ruthenium(II) modified electrodes based on nucleic acid oxidation. *Electrochem. Comm.* 9:1474–79
68. Guo Z, Dong S. 2004. Electrogenerated chemiluminescence from $Ru(bpy)_3^{2+}$ ion-exchanged in carbon nanotube/perfluorosulfonated ionomer composite films. *Anal. Chem.* 76:2683–88
69. Zhuang Y, Ju H. 2005. Determination of reduced nicotinamide adenine dinucleotide based on immobilization of tris(2,2′-bipyridyl)ruthenium(II) in multiwall carbon nanotubes/Nafion composite membrane. *Anal. Lett.* 38:2077–88
70. Choi H, Lee J, Lyu Y, Lee W. 2006. Tris(2,2′-bipyridyl)ruthenium(II) electrogenerated chemiluminescence sensor based on carbon nanotube dispersed in sol-gel-derived titania-Nafion composite films. *Anal. Chim. Acta* 565:48–55
71. Deleted in proof
72. Zhang L, Guo Z, Xu Z, Dong S. 2006. Highly sensitive electrogenerated chemiluminescence produced at $Ru(bpy)_3^{2+}$ in Eastman–AQ55D–carbon nanotube composite film electrode. *J. Electroanal. Chem.* 592:63–67
73. Li J, Xu Y, Wei H, Huo T, Wang E. 2007. Electrochemiluminescence sensor based on partial sulfonation of polystyrene with carbon nanotubes. *Anal. Chem.* 79:5439–43
74. Lin Z, Chen J, Chen G. 2008. An ECL biosensor for glucose based on carbon-nanotube/Nafion film modified glass carbon electrode. *Electrochim. Acta* 53:2396–401
75. Chang Z, Zheng X. 2006. Highly sensitive electrogenerated chemiluminescence (ECL) method for famotidine with pre-anodizing technique to improve ECL reaction microenvironment at graphite electrode surface. *J. Electroanal. Chem.* 587:161–68
76. Lin Z, Chen G. 2006. Determination of carbamates in nature water based on the enhancement of electroluminescent $Ru(bpy)_3^{2+}$ at the multi-wall carbon nanotube–modified electrode. *Talanta* 70:111–15
77. Chen J, Lin Z, Chen G. 2007. An electrochemiluminescent sensor for glucose employing a modified carbon nanotube past electrode. *Anal. Bioanal. Chem.* 388:399–407
78. Guo Z, Dong S. 2005. Electrogenerated chemiluminescence determination of dopamine and epinephrine in the presence of ascorbic acid at carbon nanotube/Nafion-$Ru(bpy)_3^{2+}$ composite film modified glassy carbon electrode. *Electroanalysis* 17:607–12
79. Wohlstadter J, Wilbur J, Sigal G, Biebuyck H, Billadeau M, et al. 2003. Carbon nanotube-based biosensors. *Adv. Mater.* 15:1184–87
80. Tao Y, Lin Z, Chen X, Huang X, Oyama M, et al. 2008. Functionalized multiwall carbon nanotubes combined with bis(2,2′-bipyridine)-5-amino-1,10 phenanthroline ruthenium(II) as an electrochemiluminescence sensor. *Sens. Actuators. B* 129:758–63
81. Bruchez M, Moronne M, Gin P, Weiss S, Alivisatos A. 1998. Semiconductor nanocrystals as fluorescent biological labels. *Science* 281:2013–16
82. Chan W, Nie S. 1998. Quantum dot bioconjugates for ultrasensitive nonisotopic detection. *Science* 281:2016–18
83. Chen S, Truax L, Sommers J. 2000. Alkanethiolate-protected PbS nanoclusters: synthesis, spectroscopic and electrochemical studies. *Chem. Mater.* 12:3864–70
84. Ding Z, Quinn B, Haram S, Pell L, Korgel B, Bard AJ. 2002. Electrochemistry and electrogenerated chemiluminescence from silicon nanocrystal quantum dots. *Science* 296:1293–97
85. Myung N, Ding Z, Bard AJ. 2002. Electrogenerated chemiluminescence of CdSe nanocrystals. *Nano Lett.* 2:1315–19
86. Myung N, Bae Y, Bard AJ. 2003. Effect of surface passivation on the electrogenerated chemiluminescence of CdSe/ZnSe nanocrystals. *Nano Lett.* 3:1053–55
87. Bae Y, Myung N, Bard AJ. 2004. Electrochemistry and electrogenerated chemiluminescence of CdTe nanoparticles. *Nano Lett.* 4:1153–61

88. Bae Y, Lee D, Rhogojina E, Jurbergs D, Korgel B, Bard AJ. 2006. Electrochemistry and electrogenerated chemiluminescence of films of silicon nanoparticles in aqueous solution. *Nanotechnology* 17:3791–97
89. Poznyak S, Talapin D, Shevchenko E, Weller H. 2004. Quantum dot chemiluminescence. *Nano Lett.* 4:693–98
90. Aldana J, Wang Y, Peng X. 2001. Photochemical instability of CdSe nanocrystals coated by hydrophilic thiols. *J. Am. Chem. Soc.* 123:8844–50
91. Liu X, Jiang H, Lei J, Ju H. 2007. Anodic electrochemiluminescence of CdTe quantum dots and its energy transfer for detection of cathecol derivatives. *Anal. Chem.* 79:8055–60
92. Yu W, Qu L, Guo W, Peng X. 2003. Experimental determination of the extinction coefficient of CdTe, CdSe, and CdS nanocrystals. *Chem. Mater.* 15:2854–60
93. Han H, Sheng Z, Liang J. 2007. Electrogenerated chemiluminescence from thiol-capped CdTe quantum dots and its sensing application in aqueous solution. *Anal. Chim. Acta* 596:73–78
94. Zhang H, Zhen Z, Yang B, Gao M. 2003. The influence of carboxyl groups on the photoluminescence of mercaptocarboxylic acid–stabilized CdTe nanoparticles. *J. Phys. Chem. B* 107:8–13
95. Jiang H, Ju H. 2007. Enzyme–quantum dots architecture for highly sensitive electrochemiluminescence biosensing of oxidase substrates. *Chem. Commun.* 404–6
96. Jiang H, Ju H. 2007. Electrochemiluminescence sensor for scavengers of hydroxyl radical based on its annihilation in CdSe quantum dots film/peroxide system. *Anal. Chem.* 79:6690–96
97. Meister A, Anderson M. 1983. Glutathione. *Annu. Rev. Biochem.* 52:711–60
98. Jie G, Zhang J, Wang D, Cheng C, Chen H, Zhu J. 2008. Electrochemiluminescence immunosensor based on CdSe nanocomposite. *Anal. Chem.* 80:4033–39
99. Jie G, Liu B, Pan H, Zhu J, Chen H. 2007. CdS nanocrystal–based electrochemiluminescence biosensor for the detection of low-density lipoprotein by increasing sensitivity with gold nanoparticle amplification. *Anal. Chem.* 79:5574–81
100. Chang Y, Palacios R, Fan F, Bard AJ, Barbara P. 2008. Electrogenerated chemiluminescence of single conjugated polymer nanoparticles. *J. Am. Chem. Soc.* 130:8906–7
101. Palacios R, Fan F, Grey J, Suk J, Bard AJ, Barbara P. 2007. Charging and discharging of single conjugated-polymer nanoparticles. *Nat. Mater.* 6:680–85
102. Palacios R, Fan F, Bard AJ, Barbara P. 2006. Single-molecule spectroelectrochemistry (SMSEC). *J. Am. Chem. Soc.* 128:9028–29
103. Fan F, Bard AJ. 2008. Observing single particle collisions by electrogenerated chemiluminescence amplification. *Nano Lett.* 8:1746–49

Annual Review of
Analytical Chemistry

Volume 2, 2009

Contents

Errata

An online log of corrections to *Annual Review of Analytical Chemistry* articles may be found at http://anchem.annualreviews.org/errata.shtml